JVSTB
JOURNAL OF VACUUM SCIENCE AND TECHNOLOGY B

Collective buckling of line arrays created by soft lithography

Ziguang Chen, Jiashi Yang, and Li Tan

Citation: J. Vac. Sci. Technol. B **29**, 021001 (2011); doi: 10.1116/1.3545808
View online: http://dx.doi.org/10.1116/1.3545808
View Table of Contents: http://avspublications.org/resource/1/JVTBD9/v29/i2
Published by the AVS: Science & Technology of Materials, Interfaces, and Processing

Collective buckling of line arrays created by soft lithography

Ziguang Chen, Jiashi Yang, and Li Tan[a)]
Department of Engineering Mechanics and Nebraska Center for Materials and Nanoscience, University of Nebraska, Lincoln, Nebraska 68588-0526

(Received 7 September 2010; accepted 26 December 2010; published 21 January 2011)

The authors analyze the collective buckling of an array of elastic lines with their lower edges built into an elastic substrate of the same material. These lines can interact among themselves through the deformation of the substrate. From the theory of elasticity and elastic structures, an eigenvalue problem is formulated and solved. Calculations show that the lines can buckle collectively into certain ordered patterns, where some of which have been confirmed by experiments. The results are useful for the understanding, design, and application of the nanostructures produced by soft lithography and other embossing techniques. © *2011 American Vacuum Society.*
[DOI: 10.1116/1.3545808]

I. INTRODUCTION

Periodic arrays of protruded columns and lines of elastic polymers can be made on a substrate of the same material by soft lithography,[1] nanoimprint lithography,[2,3] and other nanofabrication techniques.[4–6] These structures are of the order of 100 nm in dimension (diameter or width) and thermal, electrical, or magnetic fillers can be incorporated for various desired properties, leading to applications such as optical gratings,[7] sensor arrays,[8] and actuators.[9] Due to the deformability of the soft lines and the substrates, structural instability is an inherent issue in the nanofabrication process. While resulting buckling or collapsing of the soft structures[1–4,10–12] could severely affect functionalities or applications, a good understanding, prediction, and control of the buckling can lead to creative means in nanofabrication[13,14] and applications.[15,16]

The buckling of soft nanostructures has certain aspects that are different from conventional buckling in structural engineering. What is unique is that the substrates of the structures are also very compliant. Neighboring columns or lines interact through the deformation of the substrate and can buckle in a collective manner to form ordered patterns. The buckling analyses in conventional structural engineering are usually for a single column or plate,[17,18] including the buckling of a beam under its own weight,[17] the buckling of a beam lying on an elastic foundation,[18] and the lateral buckling of a high beam.[19] The results from the buckling of a single elastic beam were used to analyze the buckling of a single soft nanocolumn in soft lithography and the contact of two buckled columns,[20] but the substrate deformation and the column interaction through the substrate were not considered. Therefore those results[20] do not describe the collective buckling of the columns and can only provide limited understanding of the situation. A major progress in the buckling analysis of these soft nanostructures was recently made[4] on the buckling of an array of rigid columns on an elastic substrate. Due to the inclusion of the most basic mechanism into the theoretical model, i.e., neighboring columns interact through the deformation of the substrate, the most basic collective buckling behavior of the column array can be described, which qualitatively match experimental findings. Even though the model[4] was later generalized to cover many other cases, such as a two-dimensional array of rigid columns,[21] a nonuniform one-dimensional (1D) array of rigid columns,[22] and a one-dimensional array of elastic columns,[23] there is yet little understanding of the experimental phenomenon on soft lines forming complex buckling configurations on an elastic substrate. In this article we push the model even further by considering the variation of the buckled states along the longitudinal direction of the lines.

II. EXPERIMENTAL METHODS

Silicon grating molds with a height of 150 nm and a pitch of 200 nm were purchased from Nanonex (Monmouth Junction, NJ) and used as casting stamps in embossing/imprinting nanolithography. The elastic material used in embossing/imprinting is polydimethylsiloxane (PDMS, Sylgard 184®, viscosity of 5000 cS), a two-part silicone elastomers from Dow Corning. Other chemicals were purchased from Sigma-Aldrich and used as received. The elastic films were prepared by vigorous mixing of a 10:1 ratio of base (5.0 g) and curing agent (0.5 g) in a plastic beaker followed by degassing in a vacuum chamber. Cured elastic thin films over Si stamps were then cut into long strip (4.5×1.0 cm^2) and used as substrate for soft mold replication.

Surface features on Si mold or buckling modes in PDMS copies were investigated by atomic force microscope (AFM, Dimension 3100 and Nanoscope IIIa, Veeco). AFM images were acquired using tapping mode. A silicon microcantilever with an etched conical tip (radius of curvature of 30 nm) was used for the scanning, where the short cantilever has a nominal resonant frequency of 300 kHz and a spring constant of 40 N/m.

III. RESULTS AND DISCUSSION

A. Theoretical analysis

Figure 1(a) shows the cross section of an array of identical soft lines along x_1, the normal to the article. These lines

a)Electronic mail: ltan4@unl.edu

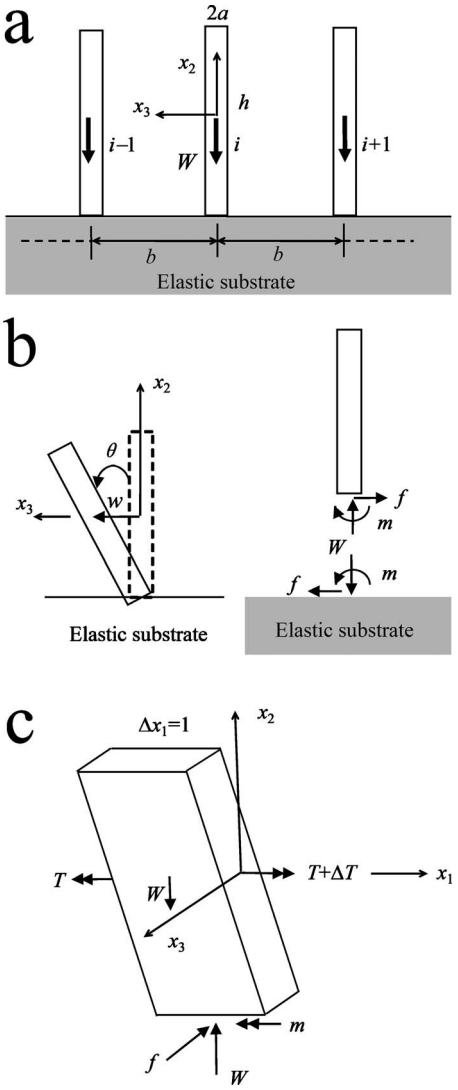

FIG. 1. Schemes for the mechanics modeling. (a) Cross section of an array of elastic lines on an elastic substrate ($h \gg 2a$), (b) deflection w and rotation angle θ of the cross section of a typical line as well as its interactions with the substrate, and (c) free body diagram for torsion of a differential element of a typical line structure.

are of infinite length, and the cross sections are rather high and thin. The weight per unit length of a single line is denoted by $W=\rho g 2ah$. In our theoretical analysis, we only consider weight as the driven force.[20,24] Although other forces including van der Waals, Coulomb, or capillary forces could also contribute to the situation,[24–26] especially when the structures are very small, these effects play rather similar role as weight or interaction coefficient as defined in our following model. Therefore, our treatment will not affect results on the buckled patterns qualitatively.

The substrate will be modeled by the theory of elasticity.[27] From the view of structural mechanics, each line on the substrate can be defined as a beam. When buckling occurs, the cross section center of a single beam undergoes a horizontal displacement w in the x_3 direction which represents bending of the beam [see Fig. 1(b)]. At the same time the cross section also rotates around the center through an angle θ which represents torsion of the beam [see Fig. 1(b)]. The beams will be modeled by the one-dimensional theories for bending and torsion.[28] In the theories of bending and torsion of beams, the cross sections of the beams are approximately rigid. Therefore, the beam cross sections shown in Fig. 1(a) are effectively the one-dimensional array of rigid columns.[4] However, our present model includes the variation of the beams along x_1 or longitudinal direction of the lines during buckling, which was not considered before.[4] Now, we allow the bottoms of the cross sections to rotate in the substrate, but neglecting their horizontal and vertical displacements as an approximation.[29] Our buckling problem will then be described by an eigenvalue problem mathematically. It is worthwhile to note that, in our previous work,[29] we found that the horizontal and vertical displacements of the beam bottoms essentially do not affect the eigenvalues and they do not affect the eigenvectors associated with the lower and higher eigenvalues either. For the eigenvectors associated with the middle eigenvalues, they only affect the order of the eigenvectors but not the eigenvectors themselves. Therefore neglecting these displacements can produce accurate interpretations.

Let us consider the bending of the beams first, where the interaction forces and moment between the bottom of a beam cross section and the substrate are shown in Fig. 1(b). Let the deflection in the x_3 direction of the centerline of the ith beam be $w^{(i)}(x_1)$ and the corresponding bending moment be $M^{(i)}(x_1)$. The Euler–Bernoulli theory for bending consists of[28]

$$M^{(i)}_{,11} - f^{(i)} = 0, \tag{1}$$

$$M^{(i)} = -\frac{2ha^3}{3} E w^{(i)}_{,11}, \tag{2}$$

where the indices after a comma denote partial differentiation with respect to the coordinate associated with the index. Equation (1) is from Newton's law in the x_3 direction, where $f^{(i)}$ is the transverse force in the x_3 direction per unit length of the beam. Equation (2) is the usual moment-curvature relation for beams, where E is the Young's modulus and is an elastic constant. Since the beams and the substrate are of the same isotropic elastic material, only two material constants are needed, where one of them (E) is relevant to the bending and the other one (μ, shear modulus) will be introduced later. Substitution of Eq. (2) into Eq. (1) gives the following equation for the deflection $w^{(i)}(x_1)$:

$$\frac{2ha^3}{3} E w^{(i)}_{,1111} + f^{(i)} = 0. \tag{3}$$

For the torsion of the beams, let the rotation of the cross section of the ith beam be $\theta^{(i)}(x_1)$ and the corresponding twisting moment be $T^{(i)}(x_1)$. We have[28]

$$T^{(i)}_{,1} - m^{(i)} + f^{(i)}\frac{h}{2} + W\frac{h}{2}\theta^{(i)} = 0, \tag{4}$$

$$T^{(i)} = C\theta_{,1}^{(i)}, \tag{5}$$

where $C=k_1\mu h^3 2a$ is the torsional rigidity of the beam (μ is the shear modulus. k_1 is a dimensionless parameter depending on the aspect ratio $2a/h$ of the cross section and can be found from a table in Ref. 28. For narrow rectangles $k_1=1/3$) and $m^{(i)}$ is the twisting moment per unit length of the beam. Physically Eq. (5) describes the balance of the twisting moments on a differential element of a typical beam [see Fig. 1(c)]. Substitution of Eq. (5) into Eq. (4) gives the equation for the rotation angle $\theta^{(i)}(x_1)$:

$$2k_1\mu h^3 a\theta_{,11}^{(i)} - m^{(i)} + f^{(i)}\frac{h}{2} + W\frac{h}{2}\theta^{(i)} = 0. \tag{6}$$

We have the following boundary condition for $w^{(i)}(x_1)$ and $\theta^{(i)}(x_1)$ stating that the horizontal displacement at the bottom of the beam is zero:

$$u_3^{(i)}|_{x_2=-h/2} = w^{(i)} - \theta^{(i)}\frac{h}{2} = 0. \tag{7}$$

In addition, we have the following relation between the rotations and moments at the bottoms of the beams:[4]

$$\theta^{(i)} = \sum_j \alpha^{(i,j)}m^{(j)} \cong \alpha^{(i,i-1)}m^{(i-1)} + \alpha^{(i,i)}m^{(i)} + \alpha^{(i,i+1)}m^{(i+1)}, \tag{8}$$

where the interaction coefficients $\alpha^{(i,j)}$ physically represent the rotation of the normal of the substrate at the ith location due to a unit moment at the jth location only, with moments at all other locations being zero. We use the same influence coefficients as in Ref. 4 as an approximation for our present case with slow variation along x_1. Equation (8) can be inverted to give[4]

$$m^{(i)} = \sum_j \beta^{(i,j)}\theta^{(j)} \cong \beta^{(i,i-1)}\theta^{(i-1)} + \beta^{(i,i)}\theta^{(i)} + \beta^{(i,i+1)}\theta^{(i+1)}, \tag{9}$$

where $\beta^{(i,j)}$ are the components of the matrix or tensor inverse of $\alpha^{(i,j)}$.

Equations (3), (6), (7), and (9) are four linear homogeneous differential equations for $w^{(i)}(x_1)$, $\theta^{(i)}(x_1)$, $f^{(i)}(x_1)$, and $m^{(i)}(x_1)$. Let

$$\begin{Bmatrix} w^{(i)}(x_1) \\ \theta^{(i)}(x_1) \\ f^{(i)}(x_1) \\ m^{(i)}(x_1) \end{Bmatrix} = \begin{Bmatrix} A^{(i)} \\ B^{(i)} \\ C^{(i)} \\ D^{(i)} \end{Bmatrix} \sin \xi x_1, \tag{10}$$

where $A^{(i)}$, $B^{(i)}$, $C^{(i)}$, $D^{(i)}$, and ξ are arbitrary constants. ξ describes the variation along x_1, where previous results[4] are for the special case of $\xi=0$. The main purpose of the present article is to study the more general case of a nonzero ξ in terms of its contribution to the complex configurations along the long direction of lines. With Eq. (10), Eqs. (3), (6), (7), and (9) become

$$\frac{2ha^3}{3}E\xi^4 A^{(i)} + C^{(i)} = 0, \tag{11a}$$

$$-2k_1\mu h^3 a\xi^2 B^{(i)} - D^{(i)} + C^{(i)}\frac{h}{2} + W\frac{h}{2}B^{(i)} = 0, \tag{11b}$$

$$A^{(i)} - B^{(i)}\frac{h}{2} = 0, \tag{11c}$$

$$D^{(i)} = \beta^{(i,i-1)}B^{(i-1)} + \beta^{(i,i)}B^{(i)} + \beta^{(i,i+1)}B^{(i+1)}. \tag{11d}$$

Equation (11) is a group of linear homogeneous equations and constitutes an eigenvalue problem. It has a trivial solution of zero representing the unbuckled state. We are interested in nontrivial solutions representing buckled states. We use Eqs. (11a), (11c), and (11d) to obtain expressions of $A^{(i)}$, $C^{(i)}$, and $D^{(i)}$ in terms of $B^{(i)}$ and substitute them into Eq. (11b) to obtain a system of linear homogeneous equations for $B^{(i)}$:

$$\beta^{(i,i-1)}B^{(i-1)} + \beta^{(i,i)}B^{(i)} + \beta^{(i,i+1)}B^{(i+1)} = \lambda B^{(i)}, \tag{12}$$

where

$$\lambda = W\frac{h}{2} - 2k_1\mu h^3 a\xi^2 - \frac{h^3a^3}{6}E\xi^4. \tag{13}$$

Then the determinant of the coefficient matrix of Eq. (12) has to vanish, which determines the eigenvalue λ. The corresponding nonzero solutions of $B^{(i)}$ (eigenvectors) determine the buckled states. We note that Eq. (12) reduces to the model in Ref. 4 when $\xi=0$. Equation (13) shows that effectively the eigenvalue $Wh/2$ in Ref. 4 is shifted due to the consideration of ξ through combined torsion and bending. As a generalization of the case of $\xi=0$ in Ref. 4, the present article is concerned with the case of nonzero and small ξ. Physically this describes slow variations along x_1 for which the beam theory is still valid. As shown in Eq. (13), when ξ is small, the effects of torsion and bending are of the orders of ξ^2 and ξ^4, respectively. Therefore, torsion has a more important role than bending. The critical value of $Wh/2$ for buckling becomes larger for larger ξ or more drastic variations along x_1, i.e., higher-order buckling modes.

B. Multiple modes of buckling

As a numerical example we consider an array of 20 beams with $a=50$ nm, $b=200$ nm, $E=1.923\times10^6$ N/m^2, $\nu=0.5$, and $\rho=1.0512$ kg/m^3. ν is the Poisson's ratio, another elastic constant which is related to E and μ. Equation (12) is solved by MATLAB, giving the 20 eigenvalues as 8.96, 8.99, 9.05, 9.13, 9.22, 9.34, 9.48, 9.63, 9.80, 9.98, 10.16, 10.36, 10.55, 10.74, 10.92, 11.08, 11.23, 11.35, 11.43, and 11.49 nN. These eigenvalues are the same as Ref. 4. For a specific eigenvalue λ, Eq. (13) determines a relationship among the geometrical and physical parameters of the beams and ξ. We will focus on the relation between h and ξ. Numerical studies show that, for a fixed λ and a fixed h, Eq. (13) has only one real and positive root for ξ. Corresponding to the first eigenvalues λ_1, when $\xi=0$, the critical height of the beam cross

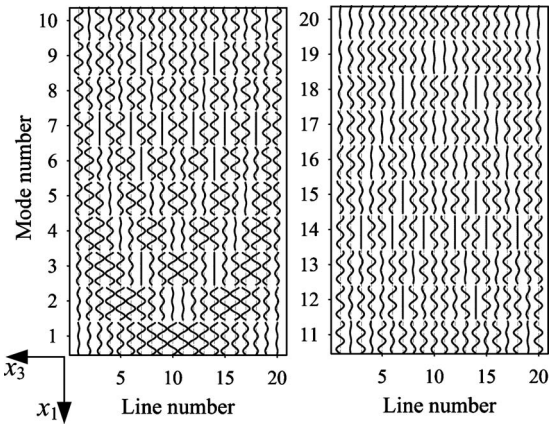

FIG. 2. Calculated modes of collective buckling on soft surface, ranked by the increasing magnitude of eigenvalues. All 20 modes are shown in this figure.

sections is found to be $h_c=\sqrt{\lambda_1/\rho g a}$. When ξ is nonzero, the critical height of the beam across sections increases according to Eq. (13). For any given $h>h_c$, the eigenvalues determine a series of values of ξ. As an example we arbitrarily choose $h=1.3h_c$ which is slightly larger than h_c. The corresponding values of ξ are 1.3585, 1.3465, 1.3345, 1.3345, 1.3223, 1.31, 1.2976, 1.2724, 1.2596, 1.2336, 1.2204, 1.1799, 1.1661, 1.138, 1.1237, 1.0945, 1.0796, 1.0645, 1.0492, and 1.0492 m^{-1}. For any other h values ($h>h_c$), the values of ξ will change, but this change will not affect the shape of the buckled lines.

Based on the corresponding eigenvectors, in Fig. 2 we plot the displacement in the x_3 direction at the top of the beams given by

$$u_3^{(i)}|_{x_2=h/2}=w^{(i)}(x_1)+\theta^{(i)}(x_1)\frac{h}{2}. \tag{14}$$

A three-dimensional (3D) plot of the buckling states is shown in Fig. 3. These figures show the variation of the buckled states along the x_1 direction which is obtained theoretically for the first time. In the first mode, two neighboring beams buckle in opposite directions, toward or away from each other. As the mode number increases, neighboring beams tend to buckle in the same direction. In the last mode, all beams buckle in the same direction.

C. Experimental verification

To appreciate the real picture of the buckling in soft lines, we used the process of embossing/imprinting lithography and created periodic lines atop an elastic material, PDMS. The soft nanostructure was formed by spin coating the PDMS precursor mixture on a rigid mold and baking at an elevated temperature for an extended period of time. In order to obtain a uniform pattern on PDMS, it is necessary to treat the rigid mold with oxygen plasma, followed by a perfluorosilane treatment in toluene ($0.2M$, 5 min). The soft nature of the PDMS and the high aspect ratio of the copied nanostructures from the mold often lead to collective buckling of the lines produced. We used AFM to evaluate the buckled

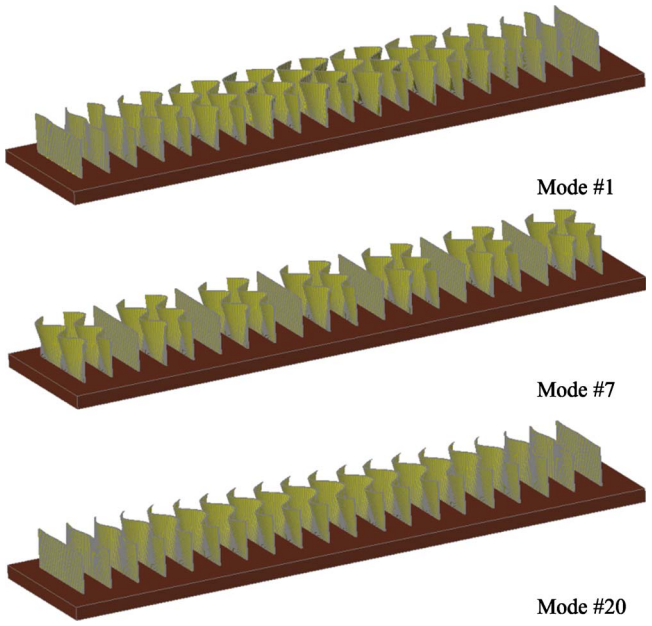

FIG. 3. (Color online) 3D structures of selected buckling modes. Top panel: mode 1, two neighboring lines buckle in opposite directions, toward or away from each other; middle panel: mode 7, several lines are not buckled; and bottom panel: mode 20, all lines buckle in the same direction.

configuration. Figure 4(a) shows the topography of the rigid stamp with 1D grating features. The resulting PDMS copies show collective buckling as in Fig. 4(b) which qualitatively matches mode 13 from the theoretical analysis. We note that theoretically the first mode in Fig. 2 corresponds to the smallest eigenvalue or minimum energy and should appear most often. However, the first mode is rarely observed in our experiments. Partially, this is because the eigenvalues are relatively close to each other, where any small fluctuations not counted in the physical parameters of those soft lines may change the order of the eigenvalues and the corresponding modes. For example, when only weight is considered, two neighboring beams prefer to buckle in opposite directions, toward or away from each other (mode 1). In contrast, when van der Waals force is involved, it will have a tendency to hold soft lines together by giving rise to line bundles. This could easily shift the buckling state from the first to the last one (mode 20). Essentially, the actual state of buckling is determined by the competition among the weight, van der Waals force, or many others. It is rather interesting to see that our buckling occurs at a state with a medium gain in energy (mode 13, as shown in the AFM images). Nevertheless, the buckled shapes between our modeling and experimental data are rather similar.

IV. CONCLUSION

A theoretical model with combined bending and torsion of thin elastic lines on an elastic substrate is established. The model can describe the collective buckling of a line array due to the interaction of the lines through the deformation of the substrate. The variation of the buckled states along the line length tends to raise the eigenvalues. Buckling in pairs

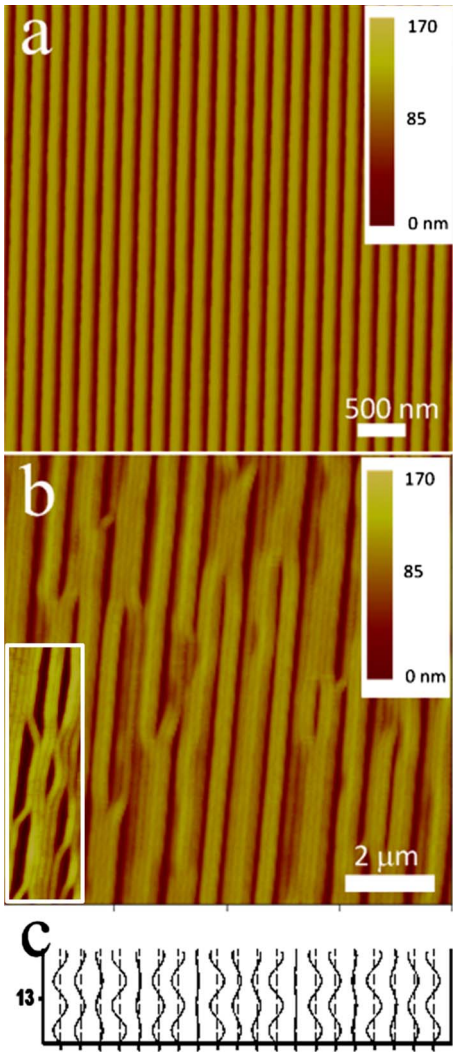

FIG. 4. (Color online) AFM topographical images of a rigid mold and fabricated PDMS structures from embossing/imprinting: (a) original mold with a pitch of 200 nm and a depth of 150 nm and (b) collective lateral buckling features, which follows mode 13 in (c). The scalar bars are 500 nm and 2 μm in (a) and (b), respectively.

with neighboring lines buckled toward or away from each other corresponds to smaller eigenvalues than the case when neighboring lines buckle in the same direction. Our work suggests that both the compliant substrate and interaction of neighboring structures through the deformation of the substrate dominate the collective buckling. This makes the buckling of periodic soft nanostructures unique and different from conventional structural engineering.

ACKNOWLEDGMENTS

L.T. gratefully acknowledges the partial financial support from the National Science Foundation (Grant No. CMMI 0825905 and 0900644) and the Army Research Office (Grant No. W911NF-08-1-0190).

[1]Y. N. Xia and G. M. Whitesides, Annu. Rev. Mater. Sci. **28**, 153 (1998).
[2]S. Y. Chou, P. R. Krauss, and P. J. Renstrom, Appl. Phys. Lett. **67**, 3114 (1995).
[3]S. Y. Chou, P. R. Krauss, and P. J. Renstrom, J. Vac. Sci. Technol. B **14**, 4129 (1996).
[4]H. J. Lin, J. S. Yang, L. Tan, J. Xu, and Z. Li, J. Phys. Chem. C **111**, 13348 (2007).
[5]C. Pina-Hernandez, L. J. Guo, and P.-F. Fu, ACS Nano **4**, 4776 (2010).
[6]Y. H. Cho, J. Park, H. Park, X. Cheng, B. J. Kim, and A. Han, Microfluid. Nanofluid. **9**, 163 (2010).
[7]H. T. Miyazaki and Y. Kurokawa, Phys. Rev. Lett. **96**, 097401 (2006).
[8]A. W. Wun, P. T. Snee, Y. T. Chan, M. G. Bawendi, and D. G. Nocera, J. Mater. Chem. **15**, 2697 (2005).
[9]A. M. Fennimore, T. D. Yuzvinsky, W. Q. Han, M. S. Fuhrer, J. Cumings, and A. Zettl, Nature (London) **424**, 408 (2003).
[10]E. Delamarche, H. Schmid, B. Michel, and H. Biebuyck, Adv. Mater. (Weinheim, Ger.) **9**, 741 (1997).
[11]H. Schmid and B. Michel, Macromolecules **33**, 3042 (2000).
[12]B. A. Evans, A. R. Shields, R. L. Carroll, S. Washburn, M. R. Falvo, and R. Superfine, Nano Lett. **7**, 1428 (2007).
[13]B. Pokroy, S. H. Kang, L. Mahadevan, and J. Aizenberg, Science **323**, 237 (2009).
[14]M. Zeng, H. L. Du, Z. G. Chen, and L. Tan, J. Phys. Chem. C **114**, 16439 (2010).
[15]D. Y. Khang, H. Jiang, Y. Huang, and J. A. Rogers, Science **311**, 208 (2006).
[16]O. Lima, L. Tan, A. Goel, M. Negahban, and Z. Li, J. Vac. Sci. Technol. B **25**, 2412 (2007).
[17]A. G. Greenhill, Proc. Cambridge Philos. Soc. **4**, 65 (1881).
[18]S. P. Timoshenko, *Theory of Elastic Stability* (McGraw-Hill, New York, 1936).
[19]N. A. Alfutov, *Stability of Elastic Structures* (Springer, Berlin, 2000).
[20]C. Y. Hui, A. Jagota, Y. Y. Lin, and E. J. Kramer, Langmuir **18**, 1394 (2002).
[21]Z. G. Chen, J. S. Yang, and L. Tan, J. Phys. Chem. B **112**, 14766 (2008).
[22]Z. Li, K. Feng, J. S. Yang, L. Tan, and H. J. Lin, Acta Mech. **209**, 285 (2010).
[23]K. Feng and Z. Li, Chin. Phys. Lett. **26**, 126202 (2009).
[24]K. G. Sharp, G. S. Blackman, N. J. Glassmaker, A. Jagota, and C. Y. Hui, Langmuir **20**, 6430 (2004).
[25]W. C. Chuang, C. T. Ho, and W. C. Wang, Opt. Express **13**, 6685 (2005).
[26]K. J. Hsia, Y. Huang, E. Menard, J. U. Park, W. Zhou, J. Rogers, and J. M. Fulton, Appl. Phys. Lett. **86**, 154106 (2005).
[27]S. P. Timoshenko and J. N. Goodier, *Theory of Elasticity* (McGraw-Hill, New York, 2007).
[28]R. D. Mindlin, Int. J. Solids Struct. **12**, 27 (1976).
[29]H. J. Lin, Z. G. Chen, J. S. Yang, and L. Tan, J. Mech. Mater. Struct. **5**, 495 (2010).